Full-length article

Body distribution and *in situ* evading of phagocytic uptake by macrophages of long-circulating poly (ethylene glycol) cyanoacrylate-co-*n*-hexadecyl cyanoacrylate nanoparticles[1]

Min HUANG, Wei WU[2], Jun QIAN, Dan-jing WAN, Xiu-li WEI, Jian-hua ZHU

School of Pharmacy, Fudan University, Shanghai 200032, China

Key words

[2] Correspondence to Assoc Prof Wei WU.
Phn 86-21-5423-7833.
Fax 86-21-6417-0921.
E-mail wuwei@shmu.edu.cn

Abstract

Aim: To investigate the body distribution in mice of [^{14}C]-labeled poly methoxyethyleneglycol cyanoacrylate-co-*n*-hexadecyl cyanoacrylate (PEG-PHDCA) nanoparticles and *in situ* evading of phagocytic uptake by mouse peritoneal macrophages. **Methods**: PEG-PHDCA copolymers were synthesized by condensation of methoxypolyethylene glycol cyanoacetate with [^{14}C]-hexadecyl-cyanoacetate. [^{14}C]-nanoparticles were prepared using the nanoprecipitation/solvent diffusion method, while fluorescent nanoparticles were prepared by incorporating rhodamine B. *In situ* phagocytic uptake was evaluated by flow cytometry. Body distribution in mice was evaluated by determining radioactivity in tissues using a scintillation method. **Results**: Phagocytic uptake by macrophages can be efficiently evaded by fluorescent PEG-PHDCA nanoparticles. After 48 h, 31% of the radioactivity of the stealth [^{14}C]-PEG-PHDCA nanoparticles after iv injection was still found in blood, whereas non-stealth PHDCA nanoparticles were cleaned up from the bloodstream in a short time. The distribution of stealth PEG-PHDCA nanoparticles and non-stealth PHDCA nanoparticals in mice was poor in lung, kidney, and brain, and a little higher in hearts. Lymphatic accumulation was unusually high for both stealth and non-stealth nanoparticles, typical of lymphatic capture. The accumulation of stealth PEG-PHDCA nanoparticles in the spleen was 1.7 times as much as that of non-stealth PHDCA (*P*<0.01). But the accumulation of stealth PEG-PHDCA nanoparticles in the liver was 0.8 times as much as that of non-stealth PHDCA (*P*<0.05). **Conclusion**: PEGylation leads to long-circulation of nanoparticles in the bloodstream, and splenotropic accumulation opens up the potential for further development of spleen-targeted drug delivery.

Introduction

One of the major objectives of advanced drug delivery today is drug targeting with colloidal drug-delivery systems, such as nanoparticles and liposomes. However, these conventional carriers are rapidly cleaned from the systemic circulation, and end almost exclusively in the mononuclear phagocyte system (MPS) after iv injection, mainly in the macrophages in the liver and spleen[1]. Of course, this extensive uptake is advantageous for treating illness of the reticuloendothelial system (RES) because it provides high local concentrations of therapeutic agents. Unfortunately, delivering drugs to sites other than RES is often desired. To meet this requirement, stealth or long-circulating nanoparticles have been investigated.

In the past two decades, there has been an increasing interest in the development of stealth nanoparticles as drug carrier systems[2,3]. One of the main methods for preparation of stealth nanoparticles is to modify their surface with a hydrophilic and non-ionic polymer, eg, poly methoxyethyleneglycol (PEG)[4] or poloxamer derivatives [5,6]. Previous studies demonstrate that the hepatic uptake of

nanoparticles can be reduced by coating these particles with certain modification. Several mechanisms are discussed for this modification of the body distribution[6,8]: a dependence on the nanoparticle surface charge, a reduction in the surface hydrophobicity reducing phagocytic uptake, a steric hindrance preventing the contact between particles and blood cells (theory of steric stabilization), and a change in the adsorption of blood components determined by the surface properties of the particles. The adsorption patterns differ depending on the physicochemical properties of the particles.

According to Peracchia *et al*, PEGylated polycyanoacrylate nanoparticles are suitable for giving iv and capable of circumventing capture by hepatic Kupffer cells[9]. The increment of splenic nanoparticles led the authors to conclude a splenic targeting mechanism. However, the investigation was taken for a duration of only 24 h, and detailed description of body distribution as a function of time in organs other than liver and spleen was absent. Other authors have studied the same vehicle by incorporating a protein drug, recombinant human tumor necrosis factor α[10]. In contrast to splenic accumulation, diversion of nanoparticles to tissues other than the liver and spleen, that is tumors, was observed.

Distribution of stealth nanoparticles to non-hepatic and non-splenic organs or tissues make them prospective vehicles for the delivery of active ingredients to these sites. In the present study, biodistribution of [14C]-labeled poly methoxyethyleneglycol cyanoacrylate-co-*n*-hexadecyl cyanoacrylate (PEG-PHDCA) nanoparticles was evaluated for the prolonged duration of 48 h. Distribution to organs other than the liver and the spleen was studied, which is also of interest for target stealth diversion. An *in situ* phagocytic evading was also investigated in mouse peritoneum using chemically induced macrophages and flow cytometry.

Materials and methods

Materials Methoxypolyethylene glycol (5000 Da of molecular weight, MePEG 5000) was obtained from Sigma Chemical Co. Cyanoacetic acid was obtained from Fluka Chemical Co and [3-14C]-cyanoacetic acid was obatined from Moravek Biochemicals. *N*, *N'*-dicyclo-hexylcarbodimide and 4-dimethylaminopyridine were obtained from Shanghai Chemical Reagent Co. Formaline (37%) was obtained from Shanghai Jianxin Chemical Co. Aqueous dimethylamine (34%) was provided by Shanghai Linfeng Chemical Co. Other reagents were of analytical purity.

Synthesis of [14C]-labeled PEGylated and non-PEGylated

PHDCA polymers Synthesis of poly PEG-PHDCA copolymers has been studied previously [11]. The PEG-PHDCA 1:3 copolymer was synthesized by condensation of MePEG 5000 cyanoacetate with [14C]-hexadecylcyanoace-tate in ethanol, in the presence of formaline and dimethylamine.

[3-14C] Cyanoacetic acid (490.4 mg, 552 μCi=20.4 MBq) was dissolved in ethyl acetate (5 mL), and a solution of hexadecanol (697.6 mg, 1.75 mmol) and 4-dime-thylamino-pyridine (1.1906 g, 1.75 mmol) in dichloromethane (9 mL) was added. Then, *N*, *N*-dicyclo-hexylcarbodimide (129.38 mg, 0.63 mmol) was added. After stirring at room temperature for 16 h, the resultant mixture was filtered. Filtrate was concentrated under vacuum, and [14C]hexadecylcyanoacetate was collected as a waxy solid (1.0386 g, 87.4%, 400 μCi=14.8 MBq). [14C] Hexadecylcyano-acetate (519.3 mg, 1.68 mmol, 200 μCi=7.4 MBq) and MePEG 5000 cyanoacetate (2.9235 g, 0.56 mmol) was added to a 1:1 mixture of ethanol and dichloro-methane (10 mL), sequentially, 37% formaline (305 μL, 3.76 mmol) and 34% aqueous dimethylamine (515 μL, 388 mmol) was added. After stirring at room temperature for 16 h, the reaction mixture was concentrated under reduced pressure. The residue was dissolved by dichloromethane (100 mL) and washed with 10 mL of water. The organic phase was dried over magnesium sulfate, and concentrated under vacuum. Non-PEGylated [14C]-polymer PHDCA was also synthesized by condensing [14C] hexadecylcyanoacetate with cyanoacetate.

Preparation of [14C]-labeled and fluorescent nanoparticles [14C]-labeled nanoparticles were prepared by a nanoprecipitation/solvent diffusion method[11]. The [14C]labeled PEG-PHDCA (1:3) copolymer (100 mg) or the [14C]PHDCA polymer was dissolved in 4 mL of tetrahydrofuran, and the polymer solution was added, under magnetic stirring, to 100 mL of demineralized water. Particle formation occurred immediately. After solvent evaporation using a rotatary evaporator, an aqueous suspension of nanoparticles (1 mg/mL) was obtained. The nanoparticles were washed twice with demineralized water after ultracentrifugation, and then filtered (Millex AP, Millopore, 1.2 μm). The radioactivity of the nanoparticle solution was determined just before injection.

Flurescent nanoparticles were prepared following similar procedures by incorporating 0.2% rhodamine B.

Characterization of nanoparticles The morphological examination of nanoparticles was performed using transmission electron microscopy (TEM) (HITACHI H-600) following negative staining with sodium phosphotungstate solution. The particle size and zeta potential of nanoparticles were determined, respectively, by photon correlation spec-

troscopy and laser Doppler anemometry (NICOMP 380/ZLS). Influence of organic solvent, polymer concentration in organic phase and preparation procedures on nanoparticle structure were previously reported[11].

***In situ* evading of phagocytic uptake by macrophages** The phagocytic evading effect of PEG-PHDCA was observed on chemically induced mouse peritoneal macrophages[12]. The mice were injected with 1 mL of 3% sodium thioglycolate solution ip as a stimulant for macrophages. After 3 d of induction, fluorescent nanoparticles were injected ip and incubated together with the macrophages for 2 h. Then, the mice were killed by cervical dislocation, and each was peritoneally injected with 5 mL of saline. The peritoneum of the mouse was massaged for 1 min and the solution inside the abdominal cavity was drawn out. Macrophages were washed 3 times with 1 mL of phosphate buffer. Cellular uptake of PEG-PHDCA nanoparticles was examined with a FACScan flow cytometer, operated under activation wavelength of 585 nm. Each assay counted 20 000 macrophages. Non-stealth PHDCA nanoparticles were also studied as a contrast, and saline as a control.

***In vivo* tissue distribution of [14C]-labeled PEG-PHDCA nanoparticles** To evaluate the body distribution of PEG-PHDCA and PHDCA nanoparticles, 2 groups of mice (6 each) at 1 time interval were treated with [14C]-PEG-PHDCA and [14C]-PHDCA nanoparticles, respectively. A total of 200 μL nanoparticle suspension at the dose of 150 mg/kg were injected into male mice (approximately 20 g in weight) through the tail vein. The amount of given radioactivity was 1.7×10^5 Bq/kg. Animals were killed after 0.05, 0.5, 3, 6, 15, 24, 36, and 48 h of injection. Meantime, blood samples were withdrawn, and hearts, livers, spleens, lungs, kidneys, brains, and lymph nodes were carefully collected. The organs were weighed immediately after removal. Alkaline tissue solubilizer (2 mol/L NaOH) was added to organ samples, and heated at 12°C for 30 min, then cooled to an ambient temperature, and 30% H_2O_2 was added with occasional swirling until the color subsided. After addition of 200 μL of acetic acid and 3 mL of scintillation cocktail (PPO/POPOP), the prepared samples were stored for approximately 2 d and then counted in the scintillation counter (LKB 1210). For determining radioactivity in blood, plasma was separated to exclude interference of blood cell lysates. Recovery of radioactivity was found to be between 95% and 103% for all tissues.

For the calculation of the radioactivity of the total dose (percentage dose) and of 1 milligram of tissue (Bq/mg), the injected radioactivity was taken as the total dose.

To evaluate the effect of specific accumulation of nanoparticles in organs, areas under the radioactivity-time curve ($AUC_{0-48 h}$) were calculated and compared.

Statistical analysis *In vivo* radioactivity values were calculated as a mean of the results of 6 mice determined separately, and presented as mean±SD. Statistical comparisons of the means were performed using multivariate analysis of variance with SARS software.

Results

Synthesis of the [14C] labeled PEGylated and non-PEGylated polymer According to our previous findings[11], PEG-polycyanoacrylate copolymers were prepared by condensation of a mixture of MePEG-cyanoacetate and *n*-hexadecyl-cyanoacetate with high yields. After standing at room temperature for 16 h and drying under vacuum, the desired copolymers were obtained as pale yellow amorphous solids. The structure and ratio between hexadecyl chains and PEG chains were confirmed by integration of the respective signals in ^{1}H-nuclear magnetic resonance (^{1}H-NMR) spectroscopy. The structure of the material was also confirmed by Fourier transform infrared spectrometer (FTIR) and the molecular weight was determined by gel permeation chromatography.

The fact that radiolabeling was integrated in the cyano group, assured a great stability of the radiolabeled copolymer. PEG-PHDCA and PHDCA were synthesized using similar techniques, only substituting MePEG-cyanoacetate for cyanoacetate.

Characterization of [14C]-labeled nanoparticles Nanoparticles prepared with PEG-PHDCA or PHDCA were spherical in shape and uniform in size of approximately 200 nm (Figure 1). PEGylated nanoparticles contrasted greatly with non-PEGylated nanoparticles, with corolla-like stains.
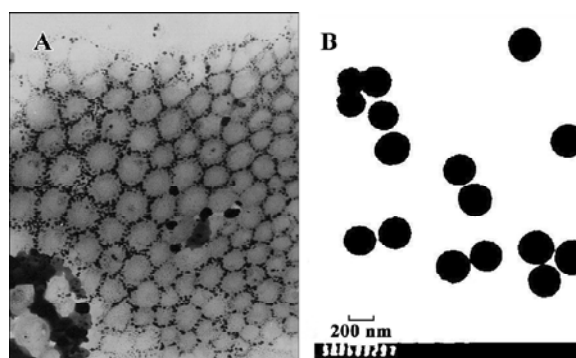

Figure 1. Transmission electron microscopy photographs of stealth PEG-PHDCA (A,×40 000) and non-stealth PHDCA (B, ×50 000) nanoparticles. PEG-PHDCA: poly methoxyethyleneglycol cyanoacrylate-co-*n*-hexadecyl cyanoacrylate. PHDCA: polyhexadecyl cyanoacrylate.

The zeta potential of PEG-PHDCA and PHDCA nanoparticles was –10.77 mV and –20.57 mV, respectively. A marked decrease in the surface charge for PEG-PHDCA nanoparticles was observed. Diameter of nanoparticles determined by photo correlation spectrometry was within the range of 188.7 nm±67.2 nm, in accordance with TEM observation.

***In situ* evading of phagotytic uptake of PEG-PHDCA nanoparticles** Incorporation of fluorescent rohodamine B in nanoparticles was verified under a research inverted system microscope (IX-71, Olympus). Loading of rhodamine B was approximately 0.2%, determined by spectrofluorometer (LS-55, PerkinElmer), upon which the assumption that toxicity of fluorescent marker to macrophages was negligible was drawn. Flow cytometry diagrams are shown in Figure 2.

The value of relative fluorescence intensity of the saline, PEG-PHDCA nanoparticles and PHDCA nanoparticles samples were 54.9, 156.5, and 1726.7, respectively, each representing the stained cells. The higher the value was, the more that the nanoparticles were captured by macrophages. Fluorescence intensity for PEG-PHDCA nanoparticles was approximately 3 times as much as that of saline control, indicating limited phagocytosis by macrophages. For non-stealth PHDCA nanoparticles, fluorescence intensity was almost 11 times as much as that of stealth PEG-PHDCA nanoparticles, indicating profound phagocytosis by macrophages. Evading of phagocytosis by macrophages was achieved through PEGylation.

Long circulating in bloodstream PEG-PHDCA nanoparticles had a remarkably higher accumulation in the bloodstream than PHDCA (*P*<0.01). PEG-PHDCA nanoparticles exhibited long-circulating characteristics, with sustained high levels of blood-associated radioactivity, and 31% of the radioactivity was still found in the bloodstream 48 h after injection, assuming that radioactivity was still associated with intact nanoparticles. In contrast, PHDCA nanoparticles were cleaned up quickly from the bloodstream, and after 30 min, dropped abruptly to a much lower level, as expected. At the end of 48 h, only approximately 4% of the radioactivity was recovered from blood (Figure 3). The PEG-PHDCA nanoparticles exhibited a 'brush' PEG configuration at the particle surface, and therefore performed the steric repulsion efficiently[13].
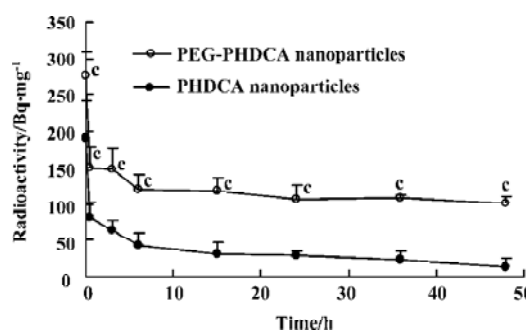
Figure 3. Blood-associated radioactivity as a function of time after iv injection of stealth PEG-PHDCA or non-stealth PHDCA nanoparticles. *n*=6. Mean±SD. ^c*P*<0.01 *vs* PHDCA nanoparticles. PEG-PHDCA: poly methoxyethyleneglycol cyanoacrylate-co-*n*-hexadecyl cyanoacrylate. PHDCA: polyhexadecyl cyanoacrylate.

Marker	% Gated	Mean
All	100.00	5.16
MI*	0.90	61.00

Marker	% Gated	Mean
All	100.00	5.36
MI*	2.69	58.19

Marker	% Gated	Mean
All	100.00	22.76
MI*	18.91	91.31

* %Gated×Mean represents overall fluorescence intensity of counted cells, with bigger values indicating increased phagocytic uptake by macrophages
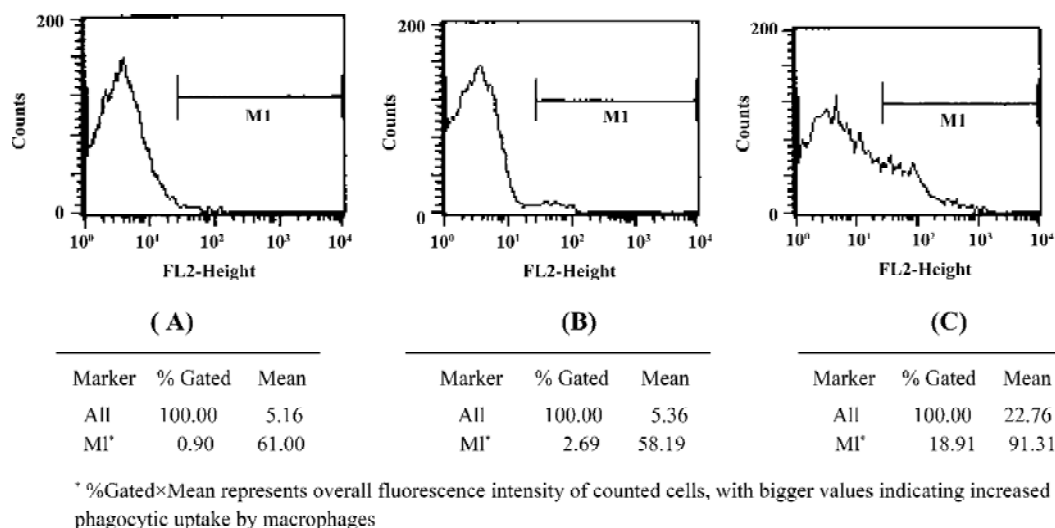
Figure 2. Flow cytometry diagrams of cellular uptake of saline (A), stealth PEG-PHDCA (B), and non-stealth PHDCA (C). PEG-PHDCA: poly methoxyethyleneglycol cyanoacrylate-co-*n*-hexadecyl cyanoacrylate. PHDCA: polyhexadecyl cyanoacrylate.

Organ accumulation The distribution of stealth PEG-PHDCA nanoparticles and non-stealth PHDCA nanoparticals in mice was poor in lung, kidney, and brain, and a little higher in heart (Table 1, Figure 4).

Table 1. $AUC_{0-48 h}$ for stealth PEG-PHDCA and non-stealth PHDCA nanoparticles in organs. AUC is the area under radioactivity-time curve. $n=6$. Mean±SD. [b]$P<0.05$, [c]$P<0.01$ *vs* non-stealth PHDCA. [e]$P<0.05$ *vs* liver. PEG-PHDCA: poly methoxyethyleneglycol cyanoacrylate-co-*n*-hexadecyl cyanoacrylate. PHDCA: polyhexadecyl cyanoacrylate.

Organ	$10^{-3} \times AUC_{stealth}/$ Bq·h·mg^{-1}	$10^{-3} \times AUC_{non-stealth}/$ Bq·h·mg^{-1}	$AUC_{stealth}/$ $AUC_{non-stealth}$
Heart	29.5±11.2	28.8±23.8	1.0
Liver	52.3±15.6[b]	69.9±19.2	0.8
Spleen	77.8±18.9[ce]	46.8±21.0[e]	1.7
Lung	22.2±8.6	27.1±13.3	0.8
Kidney	26.1±9.0	25.7±20.3	1.0
Brain	15.0±6.2	13.9±11.4	1.1
Lymph	243.9±72.0[b]	310.6±41.9	0.8
Blood	54.9±27.8[c]	15.6±2.4	3.5

There was a relatively higher accumulation in the spleen and liver for both stealth PEG-PHDCA nanoparticles and non-stealth PHDCA nanoparticals compared with heart, lung, kidney, and brain (Table 1, Figure 4).

For stealth PEG-PHDCA nanoparticles, the accumulation in the spleen was higher than that in the liver ($P<0.05$). For non-stealth PHDCA nanoparticles, the accumulation in the spleen was lower than that in the liver ($P<0.05$). The accumulation of stealth PEG-PHDCA nanoparticles in the spleen was 1.7 times as much as that of non-stealth PHDCA ($P<0.01$, Table 1, Figure 4). But the accumulation of stealth PEG-PHDCA nanoparticles in the liver was 0.8 times as much as that of non-stealth PHDCA ($P<0.05$, Table 1, Figure 4).

The amount of radioactivity of stealth PEG-PHDCA recovered from the spleen was much higher than that from liver ($P<0.01$, Figure 5). Such a high spleen uptake was also observed by other authors with PEGylated nanoparticles[9].

Accumulation in lymph nodes was unusually higher for both stealth PEG-PHDCA and non-stealth PHDCA nanoparticles compared with other organs. The radioactivity was maintained at a high level for at least 36 h, typical of lymphatic capture (Table 1). Lymphatic accumulation of stealth PEG-PHDCA was lower than that of non-stealth PHDCA nanoparticles ($P<0.05$, Figure 6).

The accumulation of stealth PEG-PHDCA nanoparticles in the blood was 3.5 times as much as that of non-stealth
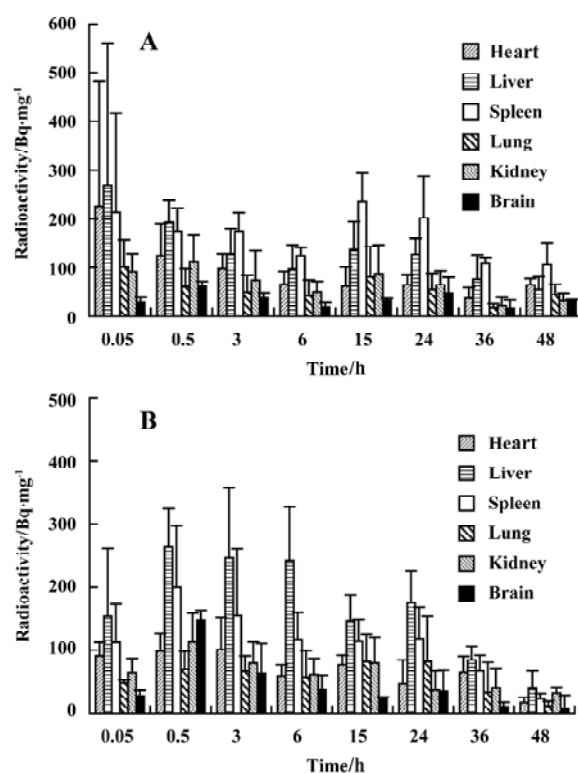

Figure 4. Tissue-associated radioactivity as a function of time after iv injection of stealth PEG-PHDCA (A) and non-stealth PHDCA (B) nanoparticles. PEG-PHDCA: poly methoxyethyleneglycol cyanoacrylate-co-*n*-hexadecyl cyanoacrylate. PHDCA: polyhexadecyl cyanoacrylate.
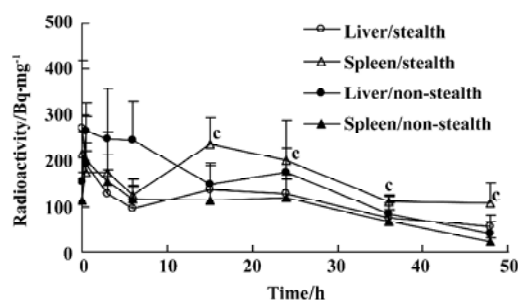

Figure 5. Spleen- and liver-associated radioactivity as a function of time after iv injection of stealth PEG-PHDCA and non-stealth PHDCA nanoparticles. $n=6$. Mean±SD. [c]$P<0.01$ *vs* Liver/stealth. PEG-PHDCA: poly methoxyethyleneglycol cyanoacrylate-co-*n*-hexadecyl cyanoacrylate. PHDCA: polyhexadecyl cyanoacrylate.

PHDCA ($P<0.01$, Table 1).

Discussion

In the present study, PEG-PHDCA was synthesized as a diblock copolymer, where PEG chains brought about hydro-
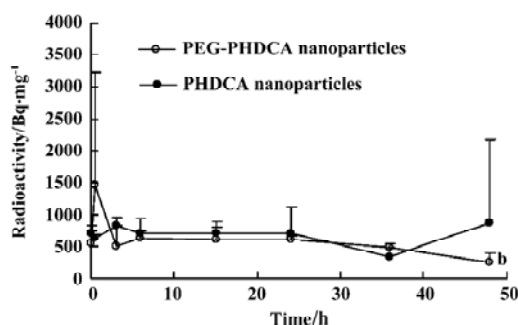
Figure 6. Lymph node-associated radioactivity as a function of time after iv injection of stealth PEG-PHDCA and non-stealth PHDCA nanoparticles. $n=6$. Mean±SD. [b]$P< 0.05$ *vs* PHDCA. PEG-PHDCA: poly methoxyethyleneglycol cyanoacrylate-co-*n*-hexadecyl cyanoacrylate. PHDCA: polyhexadecyl cyanoacrylate

philic modification of the nanoparticle surface, and hexadecyl cyanoacrylate moieties guaranteed enough hydrophobicity for the formation of nanoparticles. Structural importance was testified by ^{1}H-NMR and FTIR spectrum. Molecular weight determination by gel permeation chromatography showed a strong correlation between theoretical calculation of total amount of MePEG and hexadecyl cyanoacrylate present.

The nanoparticles were easily prepared by the nanoprecipitation/solvent diffusion method, with limited size distribution as determined by NICOMP 380/ZLS and TEM. The value of zeta potential of PEG-PHDCA nanoparticles was much lower negative than that of PHDCA nanoparticles. It should be mentioned that the PEG chains in nanoparticles would be oriented towards the outer aqueous medium, protecting the hydrophobic core. Change in surface zeta potential was also indicative of modifications by PEG chains.

Particles with hydrophobic surfaces are removed readily from the circulation through a mechanism of opsonization[6], a process involving complement adsorption and following recognition and phagocytosis by macrophages[14]. Stealth nanoparticles with "water"-like hydrophilic chains poking out interferred with adsorption of complements, and subsequent capture by macrophages. It was simple and informative to investigate interaction between vehicles and certain cell lines before taking out *in vivo* study. Stealth properties of nanoparticles have been studied *in vitro* in cultured macrophage cell lines with a fluorescent marker[15–17]. To rule out disturbing uncertainty associated with an *in vitro* method, we developed a novel *in situ* model to study the effect of stealth evading of phagocytic capture by macrophages. Preliminary results were encouraging enough for us to take out *in vivo* distribution studies.

Findings that the studied vehicles are long-circulating in the bloodstream are similar to reports by Li *et al*[10]. Sustained high levels of radioactivity of approximately one-third of the original injection for 48 h indicated longer circulation time of the vehicles, making it applicable carriers for delivering active ingredients to non-RES targets or for sustained release. Study on prolonged duration of long-circulating is needed in the future. Biodegradation of PEG-PHDCA nanoparticles has not been evaluated in the present study. However, rapid degradation was not observed in the present study, because radioactivity was embedded in the cyano groups, and if biodegradation took place, it was only associated with water-soluble small degradation remnants, which was readily eliminated from the body. For at least 48 h, nanoparticles did not undergo enormous degradation.

Splenotropic accumulation was also observed in the present study, the accumulation of stealth PEG-PHDCA nanoparticles in the spleen was 1.7 times as much as that of non-stealth PHDCA. The propensity of the mouse spleen to remove such particles from the blood was attributed to its unique architecture (reticular meshwork of the red pulp and interendothelial cell slits) and intrasplenic microcirculation (anatomically open and physiologically closed circulation)[19]. The mode of particle clearance from the blood by the spleen appeared to be initially of mechanical filtration[20]. Interestingly, large filtered sterically stabilized particles were eventually phagocytosed by the splenic red pulp macrophages[21]. Phagocytosis of such particles was, presumably, derived either as a result of intrasplenic loss of the coating, the steric barrier, or of certain intrasplenic opsonization processes. Predosing dramatically decreased the spleen uptake of splenotropic spheres but had no effect on the filtration of small sized particles (<150 nm). It is now evident that opsonization of a 'phagocyte-resistant' particle can even occur, depending on the *in vivo* circumstances. Furthermore, even stimulated macrophages can effectively recognize and internalize 'phagocyte-resistant' substrates independent of opsonization processes. Spleen-targeted stealth nanoparticles have the potential to be used to deliver nuclear substances and active components for diagnostic purposes and the therapeutic treatment of spleen-born abnormalities. In contrast, because the spleen is the biggest resident site in the human body for immune cells, such as T and B lymphocytes, delivery of vaccines into it might cause profound immunoreactions.

In summary, PEGylation leads to long-circulation of nanoparticles in the bloodstream, and splenotropic accumulation which opens up the potential for further development of spleen-targeted drug delivery.

References

1   Makino K, Yamamoto N, Higuchi K, Harada N, Ohshima H, Terada H. Phagocytic uptake of polystyrene microspheres by alveolar macrophages: effects of the size and surface properties of the microspheres. Colloid Surf B 2003; 27: 33–9.

2   Moghimi SM, Szebeni J. Stealth liposomes and long circulating nanoparticles: critical issues in pharmacokinetics, opsonization and protein-binding properties. Prog Lipid Res 2003; 42: 463–78.

3   Moghimi SM, Hunter AC, Murray JC. Long-circulating and target-specific nanoparticles: theory to practice. Pharmacol Rev 2001; 53: 283–318.

4   Neradovic D, Soga O, Nostrum CFV, Hennink WE. The effect of the processing and formulation parameters on the size of nanoparticles based on block copolymers of poly(ethylene glycol) and poly(N-isopropylacrylamide) with and without hydrolytically sensitive groups. Biomaterials 2004; 25: 2409–18.

5   Moghimi SM, Hunter AC. Poloxamers and poloxamines in nanoparticle engineering and experimental medicine. Trends Biotechnol 2000; 18: 412–20.

6   Moghimi SM. Mechanisms regulating body distribution of nanospheres conditioned with pluronic and tetronic block copolymers. Adv Drug Del Rev 1995; 16: 183–93.

7   Vandorpe J, Schacht E, Dunn S, Hawley A, Stolnik S, Davis SS, *et al*. Long circulating biodegradable poly(phosphazene) nanoparticles surface modified with poly(phosphazene)-poly (ethylene oxide) copolymer. Biomaterials 1997; 18: 1147–52.

8   Wilkins DJ, Myers PA. Studies on the relationship between the electrophoretic properties of colloids and their blood clearance and organ distribution in the rat. Br J Exp Pathol 1966; 47: 568–76.

9   Peracchia MT, Fattal E, Desmaele D, Besnard M, Noel JP, Gomis MJ, *et al*. Stealth PEGylated polycyanoacrylate nanoparticles for intravenous administration and splenic targeting. J Control Release 1999; 60: 121–8.

10 Li YP, Pei YY, Zhang XY, Gu ZH, Zhou ZH, Yuan WF, *et al*. PEGylated PLGA nanoparticles as protein carriers: synthesis, preparation and biodistribution in rats. J Control Release 2001; 71: 203–11.

11 Huang M, Wu W. Synthesis of poly [poly (ethylene glycol)-cyanoacrylate-co-hexadecyl cyanoacrylate] used for the preparation of nanoparticles. Chin J Pharm 2005; 36: 152–5.

12 Nam YS, Kang HS, Park JY, Park TG, Han SH, Chang IS. New micelle-like polymer aggregates made from PEI-PLGA diblock copolymers: micellar characteristics and cellular uptake. Biomaterials 2003; 24: 2053–9.

13 Gref R, Luck M, Quellec P, Marchand M, Dellacherie E, Harnisch S, *et al*. 'Stealth' corona-core nanoparticles surface modified by polyethylene glycol (PEG): influences of the corona (PEG chain length and surface density) and of the core composition on phagocytic uptake and plasma protein adsorption. Colloids Surf B Biointerfaces 2000; 18: 301–13.

14 Gaur U, Sahoo SK, De TK, Ghosh PC, Maitra A, Ghosh PK. Biodistribution of fluoresceinated dextran using novel nanoparticles evading reticuloendothelial system. Int J Pharm 2000; 202: 1–10.

15 Nguyen CA, Allémann E, Schwash G, Doelker E, Gurny R. Cell interaction studies of PLA-MePEG nanoparticles. Int J Pharm 2003; 254: 69–72.

16 Bocca C, Caputo O, Cavalli R, Gabriel L, Miglietta A, Gasco MR. Phagocytic uptake of fluorescent stealth and non-stealth solid lipid nanoparticles. Int J Pharm 1998; 175: 185–93

17 Illum L, Hunneyball IM, Davis SS. The effect of hydrophilic coatings on the uptake of colloidal particles by the liver and by peritoneal macrophages. Int J Pharm 1986; 29: 53–65.

18 Moghimi SM. Mechanisms of splenic clearance of blood cells and particles–towards development of splenotropic agents. Adv Drug Del Rev 1995; 17: 103–15.

19 Moghimi SM, Porter CJH, Muir IS, Illum L, Davis SS. Non-phagocytic uptake of intravenously injected microspheres in rat spleen: influence of particle size and hydrophilic coating. Biochem Biophys Res Commun 1991; 177: 861–6.

20 Moghimi SM, Hedeman H, Muir IS, Illum L, Davis SS. An investigation of the filtration capacity and the fate of large filtered sterically-stabilized microspheres in rat spleen. Biochem Biophys Acta 1993; 1157: 233–40.